THE BLACK-WHITE-BOX OPTIMIZATION NETWORK

Anonymous authors

Paper under double-blind review

ABSTRACT

We introduce a *Black–White-Box Optimization Network* and its first instance, *Tensor-Train Creator (TTC)*, which couples Ising-style solves, a factorization-machine surrogate, and tensor-train (PROTES) search. Typed couplings, lattice realignment, and warm starts cut oracle calls and time-to-target. On black-box benchmarks and Max-Cut, TTC attains better values under the same evaluation budgets.

1 Introduction

Optimization "in the wild" mixes discrete choices, hidden constraints, simulator noise, and only partially known structure. *White-box* methods exploit available structure and (possibly implicit) gradients but struggle when objectives are non-differentiable or partly unknown; *black-box* methods are flexible but often sample-hungry. We propose the **Black-White-Box Optimization Network**, a modular framework that *interleaves* white-box solvers and black-box optimizers so that each fills the other's weak points via explicit, typed couplings.

We consider problems of the form

$$\min_{x \in \mathcal{X}} f(x) \quad \text{s.t.} \quad h(x) = 0, \ g(x) \le 0, \tag{1}$$

where x may be hybrid (e.g., $x=(b,\theta)$ with $b\in\{0,1\}^n, \theta\in\mathbb{R}^m$), parts of h,g can be implicit or simulator-defined, and oracle evaluations of f are expensive and noisy.

A first instantiation: Our first Black—White-Box Optimization Network architecture—Tensor-Train Creator (TTC)—composes three building blocks: (i) an Ising-machine path (e.g., quantum/coherent annealers) as a white-box route for structured QUBO-like subproblems Yamamoto et al. (2017); dwa (2020); Osaba & Miranda-Rodríguez (2024); (ii) Higher-Order Factorization Machines (HOFM) to expose tractable low-rank polynomial structure Blondel et al. (2016); and (iii) a Tensor-Train (TT) based black-box search layer such as PROTES Batsheva et al. (2023); Oseledets (2011). Concretely, the white path solves binary subproblems

$$\min_{b \in \{0,1\}^n} \ b^{\top} Q \, b + c^{\top} b, \tag{2}$$

yielding white-box seeds that bias the TT sampler. HOFM provides a compact surrogate

$$\hat{f}(x) = w_0 + \sum_{i} w_i x_i + \sum_{k=2}^{K} \sum_{i_1 < \dots < i_k} \left\langle v_{i_1}^{(k)}, \dots, v_{i_k}^{(k)} \right\rangle \prod_{j=1}^{k} x_{i_j}, \tag{3}$$

highlighting interactions amenable to Ising-structured solves and guiding variable grouping for the search layer.

What changes in practice. Under expensive evaluations, Black–White-Box Optimization Network/TTC aims to reduce overall complexity: fewer costly oracle calls and lower time-to-target than (i) pure black-box search, (ii) pure white-box solves, or (iii) a single grey-box surrogate. We also outline how to estimate potential quantum advantage at the *systems* level—i.e., when Ising-based seeding materially lowers the number of expensive evaluations on gradient-free hard problems dwa (2020); Osaba & Miranda-Rodríguez (2024).

Contributions. (1) We formalize the **Black–White-Box Optimization Network** as a typed graph of solver nodes (black/white) with explicit couplings; (2) we present Tensor Train Creator (TTC) model, the first Black–White-Box Optimization Network architecture combining Ising-machine white solves, HOFM structure, and TT/PROTES black-box search; (3) we catalogue *architecture options* (alternative seeds, priors, and coupling operators) without changing the core graph; and (4) we provide evidence that *overall complexity decreases*, with ablations isolating the value of seeding and white-path updates.

Relation to prior work. Two-module pipelines such as **FMQA** (Factorization Machines + Quantum Annealing) motivate this design, but TTC generalizes the idea to a *network* with explicit, iterative couplings and distributional control over exploration–exploitation, accommodating hybrid variables, hidden constraints, and simulator noise Kitai et al. (2020); Endo (2025).

2 RELATED WORK

Bayesian Optimization of Function Networks (BOFN) models intermediate nodes and selects evaluations that exploit network structure Astudillo & Frazier (2021); Buathong et al. (2024). Our Black–White-Box Optimization Network retains this networked perspective while mixing heterogeneous solver types (white \leftrightarrow black), supporting typed couplings, and permitting recursion. In parallel, differentiable optimization layers such as OptNet enable implicit/argmin differentiation through solvers, which allows gradient-based "white-path" updates even when the outer objective is gradient-free Amos & Kolter (2017).

A complementary line of work orchestrates quantum and classical components: Ising machines and hybrid approaches—including Coherent Ising Machines and D-Wave's hybrid solvers—tackle combinatorial problems via cross-paradigm coordination Yamamoto et al. (2017); dwa (2020); Osaba & Miranda-Rodríguez (2024); we formalize such coordination as a *typed solver network* with explicit module interfaces. Recent two-module pipelines (e.g., FMQA) couple a factorization-machine surrogate with quantum annealing in a tight learn—propose loop Kitai et al. (2020); Endo (2025), while PROTES performs black-box optimization via tensor-train (TT) sampling to explore massive discrete spaces efficiently Batsheva et al. (2023); Oseledets (2011).

Our *TTC* framework generalizes these ideas from two-node loops to *multi-node* typed networks with principled options for seeding and mixing, and it enables white-path updates wherever nodes are differentiable.

3 THE TENSOR-TRAIN CREATOR (TTC) OPTIMIZER

We consider discrete, gradient-free black-box optimization

$$x^* \in \arg\min_{x} f(x), \qquad x = [n_1, \dots, n_d], \quad n_i \in \{1, 2, \dots, N_i\}.$$
 (4)

Before introducing TTC, we analyze *PROTES*, the TT-based component our method builds upon, clarifying both its black-box usage (treating f as an oracle) and its white-box leverage (injecting known structure directly into the TT sampler).

3.1 A TT-PARAMETERIZED SAMPLING DISTRIBUTION

PROTES (will be discussed in the next section) maintains a nonnegative *probability tensor* P (possibly unnormalized) whose entries define a sampling distribution over multi-indices. The tensor P is stored in the *tensor-train* (TT) format Oseledets (2011):

$$P[n_1, \dots, n_d] = \sum_{r_1=1}^{R_1} \dots \sum_{r_{d-1}=1}^{R_{d-1}} \mathcal{G}_1[1, n_1, r_1] \mathcal{G}_2[r_1, n_2, r_2] \dots \mathcal{G}_d[r_{d-1}, n_d, 1],$$
 (5)

with TT-cores $G_i \in \mathbb{R}^{R_{i-1} \times N_i \times R_i}$ and $R_0 = R_d = 1$. The first and last tensor cores are matrices (second order tensors) while the rest of cores are third-order tensors as shown in Figure 1. For uniform rank R, the parameter count is $O(d N R^2)$, where N is a typical mode size.

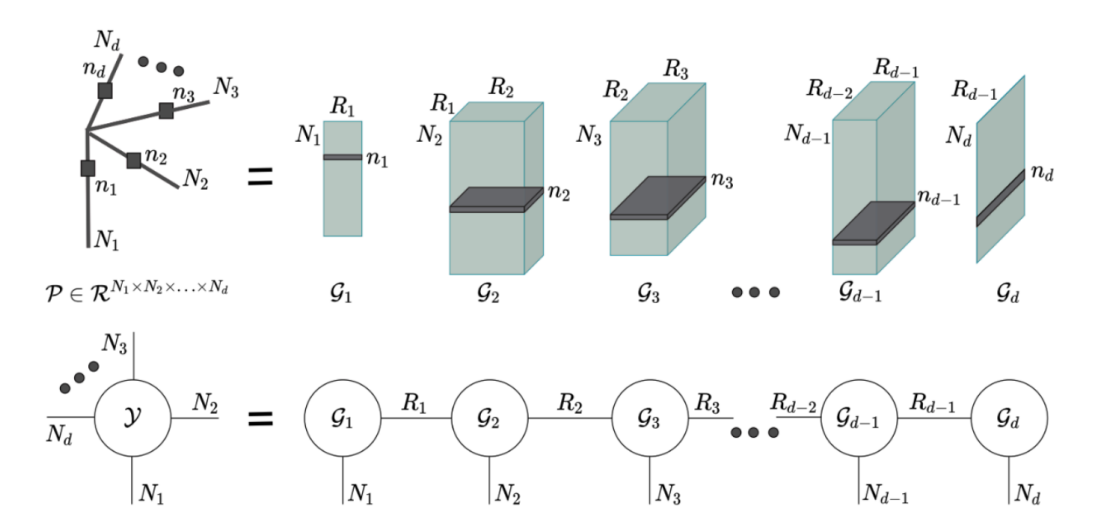


Figure 1: How the TT format works. Top: compute one entry $x[n_1, \ldots, n_d]$. Bottom: the same content as a tensor network.

In the TT format, computing $\log P[x]$ for a given multi-index x costs $O(dR^2)$ (sequential $R \times R$ matrix transfers). Additionally, one can sample from the *unnormalized* distribution P using a sequential-conditional TT sampler with time complexity

$$O(K d((N+R)R + \alpha(N)))$$
(6)

where $\alpha(N)$ is the cost of drawing from a categorical distribution with N outcomes. Both complexity results are established in Sec. 3 of the original work.

Figure 2 (Adapted from Batsheva et al. (2023), p. 3) sketches the full optimization pipeline.

3.2 PROTES: MODEL, ROLES, COMPLEXITY, AND BOTTLENECKS

The probability tensor P serves as a probability model over the search space, where each entry corresponds to the likelihood of sampling a particular combination of discrete variable values. The idea of compactly representing a multivariable probability distribution in the TT format was first proposed in Dolgov et al. (2020). The PROTES algorithm uses this compact representation and iteratively refines P by increasing probabilities for regions containing good solutions while decreasing them for poor regions, effectively concentrating sampling mass near optima. Crucially, P is stored in the tensor-train (TT) format, which provides efficient compression for high-dimensional spaces while enabling efficient sampling and updates through sequential core operations. This TT-parameterized distribution allows PROTES to navigate complex discrete optimization landscapes without requiring gradient information from the black-box objective function.

At a high level, PROTES learns a TT-structured sampler ${\cal P}$ that concentrates mass near minimizers. One iteration proceeds as follows:

- (i) Sample K candidates from P;
- (ii) Evaluate f at these candidates;
- (iii) Keep the top-k indices by objective value;
- (iv) Update P by maximizing their log-likelihood with $k_{\rm gd}$ Adam steps using automatic differentiation of $\log P[\cdot]$ through the TT cores.

Formally, with elite index set $S = \{s_1, s_2, \dots, s_k\}$ and candidates $\{x_j\}_{j=1}^K$,

$$\mathcal{L}(P; \{x_{s_i}\}) = \sum_{i=1}^{k} \log P[x_{s_i}], \tag{7}$$

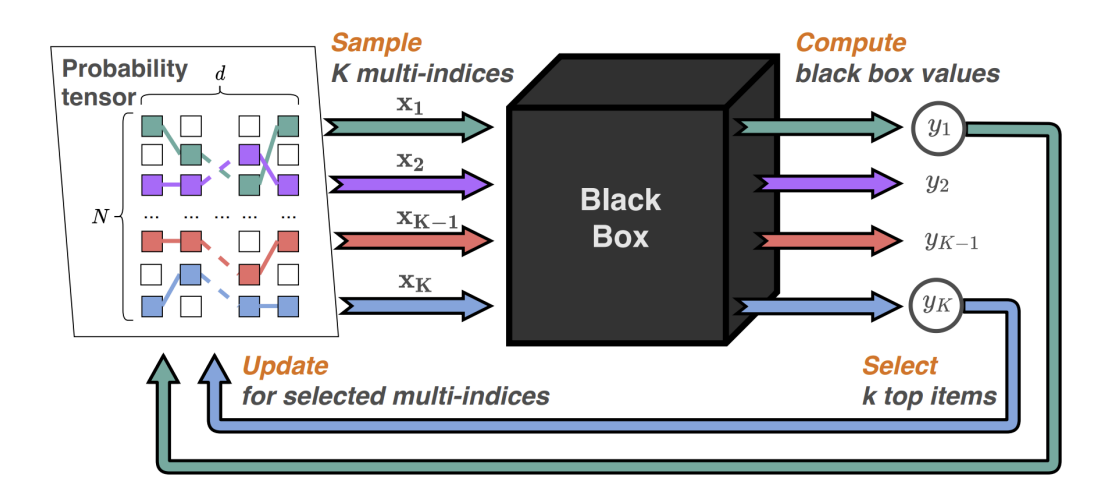


Figure 2: Conceptual outline of the PROTES optimization approach - Adapted from Batsheva et al. (2023), p. 3

which is maximized with respect to the TT parameters for $k_{\rm gd}$ steps per iteration. Although PROTES is gradient-free with respect to f, its update can be connected to the REINFORCE identity by applying a monotone transformation (e.g., Fermi–Dirac) to f. In the low-temperature limit, only elite samples contribute, yielding equation 7. Empirically, using a single hyperparameter setting ($K=100,\,k=10,\,k_{\rm gd}=1,\,\lambda=0.05,\,R=5$) across 20 diverse benchmarks leads to the best value on 19 out of 20 problems.

IS PROTES BLACK-BOX OR WHITE-BOX?

PROTES is black-box with respect to the evaluator f, because it never computes ∇f or differentiates through f; it only uses the scalar values f(x) to select an elite set S.

At the same time, each iteration solves a *white-box*, *differentiable internal subproblem* over the TT parameters θ :

$$\mathcal{L}(\theta) = \sum_{x \in S} \log P_{\theta}(x), \qquad \nabla_{\theta} \mathcal{L}(\theta) = \sum_{x \in S} \nabla_{\theta} \log P_{\theta}(x),$$

where P_{θ} is represented in Tensor-Train (TT) form and gradients are obtained by automatic differentiation through the TT cores. Thus, PROTES performs *gradient-based optimization*, but *only* on its *own model* P_{θ} (white-box), not on f (which remains black-box).

Table 1: PROTES roles with respect to the *true* objective f and the *internal* sampler P_{θ} .

Tuoic 1. Tito 12	racie 1. The TES foles with respect to the time espective f and the time sampler 1 g.				
Aspect	Role	What it means in PROTES			
Evaluator f	Black-box	No ∇f , no backprop through f ; $f(x)$ is used only to rank K candidates and pick the elite set S .			
Sampler update (P_{θ})	White-box	Optimize θ by maximizing $\sum_{x \in S} \log P_{\theta}(x)$ with gradients $\nabla_{\theta} \log P_{\theta}(x)$ through TT cores (AD).			
Known structure	White-box (optional)	Constraints/priors can be encoded directly into P_{θ} (e.g., TT indicators, structured cores), reducing wasted queries.			

Internal complexity and wall time. Let M be the number of evaluations of f (budget). Since each iteration evaluates K samples, the number of iterations is M/K.

Theorem 1 (PROTES internal time). Excluding the cost of evaluating f, one PROTES run performs

$$T_{\text{int}} = O\left(M d\left((N+R)R + \alpha(N)\right) + M d \frac{k}{K} k_{\text{gd}} R^2\right), \tag{8}$$

where $\alpha(N)$ is the cost of sampling a categorical with N outcomes.

Proof. Sequential-conditional TT sampling costs $O(K d((N+R)R + \alpha(N)))$ per iteration; over M/K iterations this yields the first term. Computing $\log P_{\theta}(x)$ and its gradient is $O(dR^2)$ per elite; over $k_{\rm gd}$ steps and k elites for M/K iterations gives the second term. See App. A for details. \square

Total wall time decomposes as

$$T_{t}$$

$$T_{\text{total}} = M T_f + T_{\text{int}}, \tag{9}$$

with T_f the average per-call latency of f. Two practical bottlenecks follow: (i) if f is expensive, M T_f dominates; (ii) the outer loop is *sequential* across iterations because the update at t+1 depends on elites from t (even though the K evaluations within each iteration can be run in parallel).

4 WHY DENSE QUBO IS HARD AND HUBO CAN BE EASIER

Empirically, reports by Batsheva et al. (2023) and follow-up experiments (e.g., Salloum 2025; Salloum et al. 2025) observe degradation on dense QUBO as dimension grows, while converting QUBO \rightarrow HUBO can improve outcomes at fixed dimension. A common misinterpretation is that "TT is better on higher-order tensors." In contrast, our analysis shows that the decisive factor is *lattice alignment*: TT/MPS complexity is governed by the size of graph/hypergraph separators along the 1D ordering, not by the algebraic order of terms.

Theorem 2 (Lattice alignment lower bound). Let $\mu(x) \propto e^{-\beta E(x)}$ be the Gibbs distribution of energy E on a graph/hypergraph G over variables (n_1, \ldots, n_d) , and let π be a 1D ordering. For every $i \in \{1, \ldots, d-1\}$, the TT bond dimension R_i required to represent μ exactly along π satisfies

$$R_i = \operatorname{rank}(\operatorname{Unfold}_i(\mu)) \ge 2^{\Omega(\operatorname{tw}_{\pi}(G,i))},$$

where $\operatorname{tw}_{\pi}(G,i)$ is the size of the minimum separator induced by the cut $(\{\pi(1),\ldots,\pi(i)\},\{\pi(i+1),\ldots,\pi(d)\})$. Moreover, the same separator controls an upper bound: $R_i \leq 2^{\operatorname{tw}_{\pi}(G,i)}$. Consequently, if G has large separators for all 1D orderings (e.g., fully connected or 2D grids), the minimal ranks grow super-polynomially with d; if G is pruned to a near-chain topology, ranks remain small.

Proof. In TT/MPS, the bond dimension R_i equals the Schmidt rank across the bipartition at position i. The Schmidt rank lower-bounds exponentially in the number of independent constraints crossing the cut. For graphical models, the number of such independent constraints scales with the size of a minimum vertex separator across the cut, i.e., the (pathwise) treewidth along π . This yields the exponential lower bound; see App. B and standard TT/MPS expressivity results Oseledets (2011). The upper bound follows by constructing a junction-tree-like contraction across a separator of size $\operatorname{tw}_{\pi}(G,i)$, implying $R_i \leq 2^{\operatorname{tw}_{\pi}(G,i)}$.

Corollary (Dense QUBO is hard). Let G be the interaction graph of a QUBO on d variables. If G is dense (e.g., $G = K_d$), then for any ordering π there exists an i with $\operatorname{tw}_{\pi}(G, i) = \Omega(d)$, hence by Theorem 2

$$R_i \geq 2^{\Omega(d)}$$
.

Therefore, exact TT representations of μ require exponentially large bond dimensions across at least one cut for every π , making dense QUBO intractable for TT-based methods.

Proof sketch. For $G = K_d$, every cut after position i has all i(d-i) cross-edges. Any separator must involve at least $\min\{i,d-i\}$ vertices, so $\operatorname{tw}_{\pi}(K_d,i) = \Omega(\min\{i,d-i\})$. Taking $i = \lfloor d/2 \rfloor$ yields $\Omega(d)$, and Theorem 2 completes the claim.

Proposition (HUBO can be easier via lattice alignment). There exist QUBO \rightarrow HUBO transformations that preserve the minimizers (and approximate the Gibbs measure on the feasible manifold) while producing a hypergraph H that admits a near-chain ordering π with $\mathrm{tw}_{\pi}(H,i) = O(w)$ for some small window w. Consequently, by Theorem 2 all TT ranks satisfy $R_i \leq 2^{O(w)}$, i.e., are polynomially bounded when w is constant or slowly growing.

Construction proof sketch. Fix a target ordering π and partition variables into contiguous blocks B_1,\ldots,B_m of size at most w. Introduce auxiliary summary bits s_b that encode prescribed local statistics of x_{B_b} , and replace dense cross-block pairwise terms by higher-order local HUBO terms within blocks plus (optionally) interactions between adjacent summaries (s_b,s_{b+1}) . Enforce s_b -consistency with HUBO penalties confined to B_b . The resulting hypergraph H has hyperedges only within blocks or between adjacent blocks, so every cut intersects O(w) variables plus O(1) summaries. Hence $\operatorname{tw}_{\pi}(H,i) = O(w)$ and $R_i \leq 2^{O(w)}$ by Theorem 2.

Examples and sanity checks. (i) All-to-all but low intrinsic rank. Energies depending only on $\sum_i x_i$ (Curie–Weiss-type) are pairwise dense but factor through a global summary. Encoding that summary as a single higher-order term aligned with π yields $\mathrm{tw}_\pi = O(1)$, so HUBO has small TT ranks. (ii) Local k-HUBO chains. If each term touches variables within a sliding window of width w along π , then $\mathrm{tw}_\pi = O(w)$ and $R_i \leq 2^{O(w)}$.

Conclusion (why dense QUBO is hard and HUBO can be easier). TT complexity is dictated by separator sizes of the *interaction lattice* along the chosen ordering, not by whether the energy is quadratic or higher-order. Dense QUBO induces large separators for all orderings, forcing $R_i \geq 2^{\Omega(d)}$ and yielding super-polynomial scaling. Converting QUBO \rightarrow HUBO can realign interactions into a near-chain hypergraph with small separators, giving $R_i \leq 2^{O(w)}$ and tractable TT compression. This explains the empirical pattern reported in Batsheva et al. (2023) and follow-up work.

Path dependence. Initialization matters because the elite-likelihood ascent increases a variational lower bound.

Theorem 3 (Initialization controls sample complexity). Fix an ordering π and rank profile (R_1, \ldots, R_{d-1}) , and let \widetilde{P} be the best TT approximation to $\mu(x) \propto e^{-\beta f(x)}$ under (π, R) . If the initial sampler P_{θ_0} satisfies $D_{\mathrm{KL}}(\widetilde{P}||P_{\theta_0}) = \Delta_0$, then elite-likelihood ascent with step size η and elite ratio k/K reduces the gap as

$$\mathbb{E}\big[\Delta_{t+1} \, \big| \, \Delta_t \big] \, \leq \, \Delta_t \Big(1 - c \, \eta \, \frac{k}{K} \Big),\,$$

for a constant c>0 depending on local smoothness and mixing, so the expected iteration count to reach $P_{\theta}(x^{\star}) \geq 1 - \varepsilon$ is $O(\Delta_0/(\eta \, k/K))$.

Proof. Write $L(\theta) = \sum_{x \in S} \log P_{\theta}(x)$ and note that $D_{\mathrm{KL}}(\widetilde{P} \| P_{\theta}) = \mathrm{const} - \mathbb{E}_{\widetilde{P}}[\log P_{\theta}(x)]$ up to approximation error. A standard smoothness argument for stochastic ascent on L with elite sampling yields linear contraction in expectation; see App. C.

Theorems 2–3 explain the QUBO/HUBO observations: converting some dense QUBO instances to HUBO can *reduce* separators (hence ranks) by inducing a near-chain hypergraph; the higher algebraic order does not harm TT if interactions remain *local* along the chain. Conversely, simply increasing ranks cannot overcome dense long-range couplings without reshaping the lattice.

4.1 THE TTC ARCHITECTURE

The *Tensor-Train Creator* (TTC) addresses two fundamental bottlenecks identified in 2–3: (i) TT ranks blow up on non–chain-like lattices, and (ii) elite-likelihood ascent is path dependent and sensitive to initialization. TTC remedies these issues by combining a higher-order factorization machine (HOFM) surrogate to expose structure, an *Ising/annealing* stage to warm-start and *shape* the surrogate lattice, and an *annealed* PROTES loop that updates the TT sampler on the true objective. The

Algorithm 1 TTC: Tensor-Train Creator

Require: budget M; initial batch B_0 ; samples/iter K; elites k; initial order $m \leftarrow 2$; annealing config (temps, reads), cooling schedule $\tau \downarrow 0$

- 1: **Seed:** draw B_0 points, evaluate f in parallel; $\mathcal{D} \leftarrow \{(x, f(x))\}_1^{B_0}$
- 328 2: while $(|\mathcal{D}| < M)$ and (not converged) do
 - 3: (Surrogate) train HOFM f_m on \mathcal{D} (few epochs)
 - (White-box) build QUBO E_{sur} from f_m (always we take the quadratic part of HOFM m=2) 4:
 - 5: (Anneal) solve E_{sur} ; obtain best \hat{z} and edge stabilities E
 - (Shape) prune weak couplings using E; contract consistent chains; get G'6:
 - 7: (TT-Create) seriate G' to get ordering π ; estimate ranks (R_i) ; init P_{θ} by moment matching
 - for $t = 1, 2, \ldots$ while budget remains and validation improves do 8:
 - 9:
 - sample K points $X_t \sim P_{\theta}^{(\tau_t)}$; evaluate $Y_t = \{f(x) : x \in X_t\}$ in parallel select elites $S_t = \arg\min_{x \in X_t}$ (top-k by f); update $\theta \leftarrow \theta + \eta \nabla_{\theta} \sum_{x \in S_t} \log P_{\theta}(x)$ 10:
 - $\mathcal{D} \leftarrow \mathcal{D} \cup \{(x, f(x)) : x \in X_t\}; \tau_{t+1} \leftarrow \gamma_\tau \tau_t$ 11:
 - 12: if (retrain period) then update f_m on current \mathcal{D} end if
- 340 13:

324

325

327

330

331 332

334

335

336

338

339

341

343 344 345

346

347

349

350

351

352 353

354

355

357

358

359

361

362

364

365

366

367

368

370 371

372

373

374 375

376 377

- if (validation plateau) then $m \leftarrow m + 1$ end if 14:
- 342 15: end while
 - 16: **return** $\arg\min_{(x,y)\in\mathcal{D}} y$

lattice is reshaped by restricting the HOFM surrogate to the relevant conditions, and the second issue is mitigated via annealing-based pruning. The ways of pruning via annealing-based solver (Ising machine) is shown in appendix E.

Pipeline. Given a budget of M black-box calls, TTC maintains a dataset \mathcal{D} , a restricted HOFM surrogate f_m of order m, a shaped interaction graph G', and a TT sampler P_θ over $\mathcal{X} = \prod_i [N_i]$. A single macro-cycle consists of:

- 1. **Parallel seeding**: evaluate an initial batch B_0 of points to form $\mathcal{D}_0 = \{(x, f(x))\}.$
- 2. **HOFM** (order m): fit \hat{f}_m with ANOVA-style factorization and chain-aware penalties; complexity per epoch is $O(m d k_{\rm H} |\mathcal{D}|)$, where $k_{\rm H}$ is the HOFM rank parameter Blondel et al. (2016).
- 3. Surrogate \rightarrow QUBO (white-box): take the m=2 part from HOFM i.e. FM.
- 4. Annealing (warm-start & shaping): solve the QUBO via an Ising backend (quantum, quantum-inspired, or GPU) to obtain solutions \hat{z} and edge stabilities. Use these to (a) warm-start the TT by moment matching of low-order marginals (reduces the initial KL gap $\Delta_0 \mapsto \Delta_1$; 3), and (b) prune/contract to produce a near-chain G' (shrinks effective ranks; 2).
- 5. TT creation & annealed PROTES: compute an ordering π by seriation on G', estimate a rank profile (R_i) from surrogate matricizations (App. D), initialize P_θ , and run an annealed PROTES loop on the true f: sample K points from $P_{\theta}^{(\tau)} \propto P_{\theta}^{1/\tau}$, evaluate f in parallel, update θ with the elite objective, augment \mathcal{D} , and periodically retrain f_m . Increase m only when validation saturates (order curriculum).

SPEED-UPS AND WHEN THEY APPEAR

Let $T_{TT}(R)$ denote the internal TT cost per f-evaluation (cf. equation 8). If annealing reduces the initialization gap by $S_{\text{init}} := \Delta_0/\Delta_1$ and the effective ranks by $\gamma \in (0,1)$ (so $R \mapsto \gamma R$), and if the annealer overhead per macro-cycle is C_{Ising} , then the internal speed-up (same black-box budget M)

$$S_{\rm int} \approx \frac{T_{\rm TT}(R)}{(\Delta_1/\Delta_0) T_{\rm TT}(\gamma R) + C_{\rm Ising}/M} \approx \frac{1}{(\Delta_1/\Delta_0) \gamma^2 + C_{\rm Ising}/(M T_{\rm TT}(R))},$$
 (10)

since the dominant TT terms scale as $O(dR^2)$. This aligns with 3 –2.

4.2 COMPLEXITY ANALYSIS

We summarize the dominant work (excluding constant factors). Let $N = \max_i N_i$; R be the nominal TT rank budget in PROTES; \bar{R} be the TTC effective rank after shaping; d be the dimension; K the samples per iteration; k the elite count; k_{gd} the ascent steps per iteration; k_{gd} the dataset size at a given time; k_{gd} the HOFM rank; and k_{gd} the cost of sampling a categorical (k_{gd} (k_{gd}) naively).

PROTES (for comparison). Internal time for a budget M is

$$T_{\text{int}}^{\text{PROTES}} = O\left(M d\left((N+R)R + \alpha(N)\right) + M d \frac{k}{K} k_{\text{gd}} R^2\right), \tag{11}$$

and total wall-time $T_{\text{tot}}^{\text{PROTES}} = M T_f + T_{\text{int}}^{\text{PROTES}}$.

FMQA (for comparison). Per outer iteration: (i) fit FM/HOFM on \mathcal{D} in $O(m d k_H T)$ per epoch; (ii) solve the surrogate by annealing with overhead C_{Ising} ; (iii) evaluate a small batch on f. If E_m epochs and B_{fm} new points per iteration, then over M evaluations (about M/B_{fm} iterations):

$$T_{\rm int}^{\rm FMQA} = O\left(\underbrace{\sum_{\rm iters} E_m \, m \, d \, k_{\rm H} \, T}_{\rm surrogate \, training} + \underbrace{\left(M/B_{\rm fm}\right) C_{\rm Ising}}_{\rm annealing \, solves}\right), \quad T_{\rm tot}^{\rm FMQA} = M \, T_f + T_{\rm int}^{\rm FMQA}. \tag{12}$$

FMQA has no TT terms but relies more heavily on annealing and surrogate quality.

TTC (this work). TTC's internal cost over a budget M decomposes into

TT sampling :
$$O(M d((N + \bar{R})\bar{R} + \alpha(N))),$$
 (13)

TT updates:
$$O\left(M d \frac{k}{K} k_{\rm gd} \bar{R}^2\right)$$
, (14)

HOFM training:
$$O\left(\sum_{\text{macro-cycles}} E_m \, m \, d \, k_{\text{H}} \, T\right)$$
, (15)

Annealing & shaping:
$$O\left(\sum_{\text{macro-cycles}} C_{\text{Ising}}\right)$$
, (16)

with $\bar{R} = \gamma R$ and an *iteration* contraction factor of about Δ_1/Δ_0 from the warm-start (3). Aggregating:

$$T_{\text{int}}^{\text{TTC}} = O\left(M d\left((N + \bar{R})\bar{R} + \alpha(N)\right) + M d \frac{k}{K} k_{\text{gd}} \bar{R}^2 + \sum_{\text{cycles}} E_m m d k_{\text{H}} T + \sum_{\text{cycles}} C_{\text{Ising}}\right). \tag{17}$$

Total wall-time:

$$T_{\text{tot}}^{\text{TTC}} = M T_f + T_{\text{int}}^{\text{TTC}}.$$
 (18)

Interpretation. Compared to equation 11, TTC replaces R by $\bar{R} = \gamma R$ in all TT terms and benefits from faster concentration in practice (fewer effective PROTES iterations to a target quality by 3). The additional costs are the *surrogate* terms equation 15 and *annealing* terms equation 16. When (i) M is moderate/large; (ii) shaping is effective ($\gamma \ll 1$); and (iii) C_{Ising} is amortized (batched reads), the reduction in the dominating $O(dR^2)$ TT terms outweighs surrogate/annealing overheads, yielding the internal speed-up in equation 10.

4.3 COMPLEXITY COMPARISON

Let $\Theta_{TT}(R) := d((N+R)R + \alpha(N)) + d\frac{k}{K}k_{gd}R^2$ denote the per-evaluation TT work. The principal internal and total costs are:

Method	Internal time	Total time		
PROTES	$M\Theta_{TT}(R)$	$M T_f + M \Theta_{TT}(R)$		
FMQA	$\sum E_m m d k_{\rm H} T + (M/B_{\rm fm}) C_{\rm Ising}$	$M T_f + \sum E_m m d k_{ m H} T + (M/B_{ m fm}) C_{ m Ising}$		
TTC (ours)	$M \Theta_{TT}(\bar{R}) + \sum E_m m d k_H T + \sum C_{Ising}$	$MT_f + M\Theta_{TT}(\bar{R}) + \sum E_m m dk_H T + \sum C_{Ising}$		

Here $\bar{R}=\gamma R$ with $\gamma\in(0,1)$ determined by lattice shaping; the *iteration* count to reach a target is reduced proportional to Δ_0/Δ_1 by warm-starting (3). Thus TTC's internal advantage over PROTES scales like γ^{-2} (rank shrink) multiplied by $S_{\rm init}=\Delta_0/\Delta_1$ (fewer effective TT iterations), up to the additive surrogate/annealing terms.

When TTC wins. If M is dominated by TT work (cheap f) and $\gamma \ll 1$, the \bar{R}^2 term reduction drives clear wins. If f is expensive, all methods share the same M T_f , so the method that reduces required M to reach a target wins; TTC does so via better initialization and lattice alignment.

ESTIMATING SYSTEMS-LEVEL QUANTUM ADVANTAGE FROM ISING-BASED SEEDING

Consider a baseline run requiring M_0 oracle evaluations with per-call latency T_f . Let the TT internal work per evaluation be

$$\Theta_{\mathrm{TT}}(R) := d\left((N+R)R + \alpha(N)\right) + d\,\frac{k}{K}\,k_{gd}\,R^2.$$

With Ising-based seeding, suppose the evaluation count shrinks by a factor $\rho \in (0,1)$ and effective ranks contract as $R \mapsto \bar{R} = \gamma R$ with $\gamma \in (0,1)$. Let $\overline{C}_{\mathsf{HOFM+Ising}}$ be the total overhead of surrogate training and seeding (including the annealer time-to-solution).

Systems-level win condition. TTC with Ising seeding improves total wall time over baseline whenever

$$M_0 \left[(1 - \rho) T_f + \Theta_{\rm TT}(R) - \rho \Theta_{\rm TT}(\bar{R}) \right] > \overline{C}_{\rm HOFM+Ising}$$
 (†)

Useful thresholds. Define $\bar{c} := \overline{C}_{HOFM+Ising}/M_0$.

$$T_f > T_f^{\star} := \frac{\bar{c} - \left(\Theta_{\mathrm{TT}}(R) - \rho \,\Theta_{\mathrm{TT}}(\bar{R})\right)}{1 - \rho}, \qquad M_0 > M_{\mathrm{min}} := \frac{\overline{C}_{\mathrm{HOFM+Ising}}}{(1 - \rho) \, T_f + \Theta_{\mathrm{TT}}(R) - \rho \,\Theta_{\mathrm{TT}}(\bar{R})}.$$

Interpreting ρ and γ . Warm-start quality controls ρ (fewer expensive evaluations); rank shaping controls γ (cheaper internal work). A crude rule of thumb is $\Theta_{\rm TT}(\bar{R}) \approx \gamma^2 \, \Theta_{\rm TT}(R)$, yielding extra headroom $(1-\rho\gamma^2)\Theta_{\rm TT}(R)$ to pay for seeding overheads.

Quantum advantage. If quantum seeding has lower total overhead than classical seeding, i.e. $\overline{C}_{\text{HOFM+Ising}}^{(Q)} < \overline{C}_{\text{HOFM+Ising}}^{(C)}$, and also satisfies (†) with the same ρ, γ , then a *systems*-level quantum advantage is achieved by materially reducing the number of expensive oracle calls.

5 Numerical Results

Table 2: Results by problem and algorithm. Row minima (in TTC, except Schwefel) are in **bold**. Values use two decimals for $|x| \ge 10^{-2}$, and scientific notation with two significant digits for $|x| < 10^{-2}$.

Problem / Algorithm	TTC	Protes	BS1 (DE)	BS2 (PSO)
ackley	4.44×10^{-16}	0.78	4.30×10^{-3}	9.10×10^{-8}
rastrigin	2.00	12.00	31.18	5.99
griewank	0.04	0.11	0.43	0.05
rosenbrock	1800.00	5942.00	2578.00	1897.00
schwefel	-402.00	-401.20	-398.00	-399.50
michalewicz	-45.50	-32.11	-45.10	-41.23
levy	5.90	10.39	7.84	5.98
max-cut	-12686.30	-10367.80	-11123.40	-10012.90

6 CONCLUSION

TTC formalizes typed couplings and fixes TT bottlenecks, translating into faster convergence and fewer evaluations than PROTES and classical baselines. Limits include surrogate quality and annealer overhead; future work adds richer node types and sharper rank/ordering estimates.

REFERENCES

- D-wave hybrid solver service: An overview. Technical report, D-Wave Systems Inc., 2020. URL https://www.dwavequantum.com/resources/white-paper/d-wave-hybrid-solver-service-an-overview/. White paper.
- Tameem Albash and Daniel A. Lidar. Adiabatic quantum computation. *Reviews of Modern Physics*, 90:015002, 2018.
- Boris Altshuler, Hari Krovi, and Jérémie Roland. Anderson localization makes adiabatic quantum optimization fail. *Proceedings of the National Academy of Sciences of the United States of America*, 107(28):12446–12450, 2010.
- Brandon Amos and J. Zico Kolter. OptNet: Differentiable optimization as a layer in neural networks. In Doina Precup and Yee Whye Teh (eds.), *Proceedings of the 34th International Conference on Machine Learning*, volume 70 of *Proceedings of Machine Learning Research*, pp. 136–145. PMLR, 06–11 Aug 2017. URL https://proceedings.mlr.press/v70/amos17a.html
- Raul Astudillo and Peter I. Frazier. Bayesian optimization of function networks. In Advances in Neural Information Processing Systems, volume 34, 2021. URL https://papers.neurips.cc/paper_files/paper/2021/file/792c7b5aae4a79e78aaeda80516ae2ac-Paper.pdf.
- F. Barahona. On the computational complexity of ising spin glass models. *Journal of Physics A: Mathematical and General*, 15:3241–3253, 1982.
- Anastasia Batsheva, Andrei Chertkov, Gleb Ryzhakov, and Ivan Oseledets. Protes: Probabilistic optimization with tensor sampling. In *Advances in Neural Information Processing Systems* (*NeurIPS*), 2023. Also available as arXiv:2301.12162.
- Mathieu Blondel, Akinori Fujino, Naonori Ueda, and Masakazu Ishihata. Higher-order factorization machines. In *Advances in Neural Information Processing Systems (NeurIPS)*, volume 29, 2016. URL https://papers.nips.cc/paper/6144-higher-order-factorization-machines.
- Poompol Buathong, Jiayue Wan, Raul Astudillo, Sam Daulton, Maximilian Balandat, and Peter I. Frazier. Bayesian optimization of function networks with partial evaluations. In Ruslan Salakhutdinov, Zico Kolter, Katherine Heller, Adrian Weller, Nuria Oliver, Jonathan Scarlett, and Felix Berkenkamp (eds.), *Proceedings of the 41st International Conference on Machine Learning*, volume 235 of *Proceedings of Machine Learning Research*, pp. 4752–4784. PMLR, 21–27 Jul 2024. URL https://proceedings.mlr.press/v235/buathong24a.html.
- Elizabeth Crosson and Aram W. Harrow. Simulated quantum annealing can be exponentially faster than classical simulated annealing. In 2016 IEEE 57th Annual Symposium on Foundations of Computer Science (FOCS), 2016.
- Elizabeth Crosson and Aram W. Harrow. Rapid mixing of path integral monte carlo for 1d stoquastic hamiltonians. *Quantum*, 5:395, 2021.
- Sergey Dolgov, Karim Anaya-Izquierdo, Colin Fox, and Robert Scheichl. Approximation and sampling of multivariate probability distributions in the tensor train decomposition. *Statistics and Computing*, 30(3):603–625, 2020.
- Kosuke Endo. Function smoothing regularization for precision factorization machine quantum annealing. *Physical Review Research*, 7(1):013149, 2025. doi: 10.1103/PhysRevResearch.7. 013149.
- Hayato Goto, Kazuyuki Tatsumura, and Andrew R. Dixon. Combinatorial optimization by simulating adiabatic bifurcations in nonlinear hamiltonian systems. *Science Advances*, 5(4):eaav2372, 2019.

- Hayato Goto, Kazuyuki Tatsumura, Issei Yanagisawa, Kenta Takemoto, Yohei Hayashi, Yasuhiko Kawabata, Yuki Uchikawa, and Kazuyuki Aihara. High-performance combinatorial optimization based on classical mechanics. *Science Advances*, 7:eabe7953, 2021.
- Bruce Hajek. Cooling schedules for optimal annealing. *Mathematics of Operations Research*, 13 (2):311–329, 1988.
- Sabine Jansen, Mary Beth Ruskai, and Ruedi Seiler. Bounds for the adiabatic approximation with applications to quantum computation. *Journal of Mathematical Physics*, 48:102111, 2007.
- Teppei Kanao and Hayato Goto. Simulated bifurcation assisted by thermal fluctuation. *Communications Physics*, 5:153, 2022.
- Koki Kitai, Jiang Guo, Jun Otsuka, Masayuki Ohzeki, Akira Miki, and Ryo Tamura. Designing metamaterials with quantum annealing and factorization machines. *Physical Review Research*, 2 (1):013319, 2020. doi: 10.1103/PhysRevResearch.2.013319.
- David A. Levin, Yuval Peres, and Elizabeth L. Wilmer. *Markov Chains and Mixing Times*. American Mathematical Society, 2 edition, 2017.
- Eneko Osaba and Pablo Miranda-Rodríguez. D-wave's nonlinear-program hybrid solver: Description and performance analysis. *arXiv* preprint arXiv:2410.07980, 2024.
- Ivan V. Oseledets. Tensor-train decomposition. SIAM Journal on Scientific Computing, 33(5):2295–2317, 2011. doi: 10.1137/090752286.
- Troels F. Rønnow, Zhihui Wang, James Job, Sergio Boixo, Sergei V. Isakov, David Wecker, John M. Martinis, Daniel A. Lidar, and Matthias Troyer. Defining and detecting quantum speedup. Science, 345:420–424, 2014.
- Yoshihisa Yamamoto, Timothée Leleu, Ken-ichi Kawarabayashi, Satoshi Kako, Martin Fejer, Kyo Inoue, and Hiroki Takesue. Coherent ising machines—optical neural networks operating at the quantum limit. *NPJ Quantum Information*, 3:49, 2017. doi: 10.1038/s41534-017-0048-9.

A PROTES: SAMPLING/UPDATE COSTS AND PROOFS

A.1 SEQUENTIAL-CONDITIONAL TT SAMPLING

The sampler generates $x_1 \sim P(n_1)$, then $x_2 \sim P(n_2 \mid n_1)$, etc., using left/right messages computed by contracting TT cores. For each step, evaluating conditionals costs O((N+R)R); sampling a categorical costs $\alpha(N)$. Over K draws and d dimensions, the sampling cost per iteration is $O(K d((N+R)R + \alpha(N)))$.

A.2 GRADIENT OF THE ELITE LOG-LIKELIHOOD

For any index x, evaluating $\log P_{\theta}(x)$ is $O(dR^2)$ via forward contractions; reverse-mode backprop through cores is the same order. Over k elites and $k_{\rm gd}$ steps per iteration, the update cost is $O(k_{\rm gd} \, k \, dR^2)$. Summing across M/K iterations proves Theorem 1.

B Lattice Alignment: Proofs of Theorems 2

For an ordering π , the TT bond dimension R_i equals the matrix rank of the unfolding across the cut $(\{1:i\}, \{i+1:d\})$. Interpreting P_{θ} as an MPS and μ as a target state, R_i equals the Schmidt rank across that bipartition. In a graphical model on G, the conditional dependence across the cut is controlled by the size of a minimal separator S_i . If $|S_i|$ grows with d, then the number of independent constraints across the cut grows, implying $R_i \geq 2^{\Omega(|S_i|)}$ for exact representation. This gives Theorem 2.

C INITIALIZATION AND KL CONTRACTION: PROOF OF THEOREM 3

Let \widetilde{P} be the best TT approximation under (π,R) and define $\Phi(\theta)=\mathbb{E}_{x\sim\widetilde{P}}[\log P_{\theta}(x)]$. Then $D_{\mathrm{KL}}(\widetilde{P}\|P_{\theta})=\mathrm{const}-\Phi(\theta)$. Elite-likelihood ascent implements a noisy ascent on Φ (up to a temperature scaling) with step size η and sampling ratio k/K. Assuming local smoothness and a Polyak-Łojasiewicz condition in a neighborhood of $\theta^{\star}=\arg\max\Phi$, the standard SGD recursion gives $\mathbb{E}[\Phi(\theta_{t+1})-\Phi(\theta_t)]\geq c\,\eta\,\frac{k}{K}\left(\Phi^{\star}-\Phi(\theta_t)\right)$, for a constant c>0, hence geometric contraction of the gap and the stated iterations bound.

D RESTRICTED HOFM, QUBO EXTRACTION, AND TT CREATION

D.1 HOFM TRAINING AND COMPLEXITY

The ANOVA trick Blondel et al. (2016) computes all orders 2:m interactions in O(m d k) passes per sample using DP recurrences, yielding O(m d k T) per epoch for dataset size T. Chain-aware group sparsity penalizes interactions far in the current ordering.

D.2 SURROGATE \rightarrow QUBO (WHITE-BOX)

For $m{=}2$, one-hot encodings yield a QUBO directly. For $m{>}2$, quadratize by introducing auxiliary variables u and penalties λ such that monomials $\prod_{i \in S} z_i$ are represented by u_S with constraints $u_S = z_{i_1} \wedge \cdots \wedge z_{i_{|S|}}$, producing $E_{\text{sur}}(z,u) = z^\top Qz + \lambda$ penalty(z,u).

D.3 ORDERING AND RANK ESTIMATION

Given a pruned graph G', obtain an ordering π via seriation (e.g., spectral ordering). Estimate a rank profile (R_i) by inspecting singular spectra of surrogate matricizations across the cuts i and selecting minimal R_i meeting an energy threshold (Tikhonov-stabilized).

D.4 MOMENT-MATCHING INITIALIZATION AND ANNEALED SAMPLING

From best surrogate solutions, build univariate and adjacent-pair marginals along π and initialize TT cores to match them at moderate inverse temperature β . Use tempered TT sampling $P_{\theta}^{(\tau)} \propto P_{\theta}^{1/\tau}$ with $\tau \downarrow 0$ to balance exploration/exploitation.

E ANNEALER-GUIDED CONVERSION OF A 2D QUBO TO A STRICT 1D NEAREST-NEIGHBOR QUBO

In this section, We present a practical pipeline that converts a quadratic unconstrained binary optimization (QUBO) defined on a 2D grid into a *strict 1D nearest-neighbor* (NN) QUBO suitable for line-structured Ising hardware. The method is *annealer-guided*: (i) obtain a reference optimum by annealing the original instance, (ii) *select* only the most valuable long-range couplers to embed exactly using equality-chain ancillas, under a user-specified ancilla budget, and (iii) prune or fold the remaining long-range interactions while preserving fidelity to the original optimum in both energy and configuration. We provide precise inputs/outputs, core identities, two selection strategies (greedy and one-shot knapsack), a penalty sweep to calibrate equality strength, and implementable pseudocode.

E.1 PROBLEM STATEMENT, INPUTS, AND OUTPUTS

Original QUBO.

$$E(x) = x^{t} opQ x + q^{t} opx + c, x \in \{0, 1\}^{n}, (19)$$

with $Q \in \mathbb{R}^{n \times n}$ (w.l.o.g. upper triangular, $Q_{ii} = 0$), $q \in \mathbb{R}^n$, and $c \in \mathbb{R}$, arranged on a 2D grid.

Inputs.

- QUBO coefficients (Q, q, c) and variable \rightarrow grid mapping.
- Access to an annealer ANNEAL $(Q, q, c; \cdot)$ returning best energy and sample.
- A line ordering $p: \{0, \ldots, n-1\} \rightarrow \{0, \ldots, n-1\}$ (e.g., snake/Hilbert).
- \bullet Ancilla budget K (maximum total chain length allowed for embeddings).
- Equality-penalty seed M_0 and a small sweep set, e.g., $\{M_0, 2M_0, 4M_0\}$.
- Pruning policy for non-embedded long edges: drop or fold.

Outputs.

- A strict 1D NN QUBO (Q', q', c') (including ancillas).
- Final annealed solution $(x_{\text{final}}, E_{\text{final}})$ on (Q', q', c').
- Selected set $S \subseteq \mathbb{E}_{far}$ of long edges embedded exactly; total ancillas $\leq K$.

E.2 PRELIMINARIES: LINE ORDER AND EDGE CLASSES

Let p be the chosen permutation (grid \rightarrow line) and define pos(i) = p(i). Partition the quadratic terms:

$$= \{(i,j) : pos(i) - pos(j) = 1, i < j\}, \qquad \mathbb{E}_{far} = \{(i,j) : pos(i) - pos(j) > 1, i < j\}.$$

For a long-range ("far") edge e=(i,j), the *chain length cost* (ancillas needed to route it along the line) is

$$L_e = pos(i) - pos(j) - 1.$$
 (20)

E.3 PRUNING POLICIES FOR LONG EDGES

For a far term $Q_{ij}x_ix_j$ we consider two simple policies:

• **drop:** remove the term.

702 • **fold** (energy-guided, using the reference optimum x^*):

 $Q_{ij}x_ix_j \approx Q_{ij} \Big(x_i \, x_i^* + x_j \, x_i^* - x_i^* x_i^* \Big). \tag{21}$

This replacement adds linear terms in x_i, x_j plus a constant, preserving strict 1D NN topology.

E.4 EXACT 1D NN EMBEDDING VIA EQUALITY CHAINS

For a selected far edge e=(i,j), let the line path be $i=v_0,v_1,\ldots,v_L=j$. Introduce ancillas z_1,\ldots,z_{L-1} and enforce *equality* along adjacent nodes using the purely quadratic penalty:

$$(u,v) = M(u-v)^2 = M(u+v-2uv), (22)$$

applied to links $(x_{v_0}, z_1), (z_1, z_2), \dots, (z_{L-1}, x_{v_L})$. At the minimum (for M large enough), $x_{v_0} = z_1 = \dots = z_{L-1} = x_{v_L}$, so we can *replace* the far quadratic by a *local* linear term on any chain node:

$$Q_{ij} x_i x_j \longrightarrow Q_{ij} z_m, \qquad m \in \{1, \dots, L-1\}.$$
 (23)

All quadratics remain NN along the line; the model stays a pure QUBO.

E.5 REFERENCE OPTIMUM BY ANNEALING

We first solve the original instance by annealing to obtain a target optimum:

$$x^* \in \underset{x \in \{0,1\}^n}{\operatorname{arg \, min}} E(x), \qquad E^* = E(x^*).$$
 (24)

This pair (x^*, E^*) guides selection and (if used) folding equation 21.

E.6 SELECTION STRATEGIES FOR LONG EDGES

We propose two annealer-guided strategies to pick a budgeted subset $S \subseteq \mathbb{E}_{far}$ to embed exactly.

E.6.1 GREEDY ANNEALER-GUIDED SELECTION (ITERATIVE)

Maintain a current embedded set S and its best annealed energy E_S for the strict 1D NN model that embeds S (and prunes others by the chosen policy). For any candidate $e \in \mathbb{E}_{far} \setminus S$, let $E_{S \cup \{e\}}$ be the best annealed energy when e is added (embedded via equation 22–equation 23). Define the *gain* per ancilla

$$g_e = \frac{E_S - E_{S \cup \{e\}}}{L_e}. (25)$$

Greedily add the edge with largest g_e while the total chain length $\sum_{f \in S} L_f$ stays within budget K, and stop when the best g_e drops below a small threshold.

E.6.2 ONE-SHOT ANNEALED VALUES + KNAPSACK

Build the *base* strict 1D NN model that keeps and prunes all far edges per policy, and anneal it to get E_{\varnothing} . For each $e \in \mathbb{E}_{far}$, build the model that embeds *only* e (on top of the base), anneal to get $E_{\{e\}}$, and define its annealed value:

$$v_e := E_{\varnothing} - E_{\{e\}} \ (\geq 0 \text{ when helpful}). \tag{26}$$

Select S by solving the 0–1 knapsack

$$\max_{y \in \{0,1\}^{|\mathbb{E}_{far}|}} \sum_{e \in \mathbb{E}_{far}} v_e y_e \quad \text{s.t.} \quad \sum_{e \in \mathbb{E}_{far}} L_e y_e \le K, \tag{27}$$

or its QUBO encoding

$$\min_{y \in \{0,1\}^{|\mathbb{E}_{far}|}} -\sum_{e} v_e \, y_e \, + \, \lambda \Big(\sum_{e} L_e \, y_e - K \Big)^2, \tag{28}$$

with $\lambda > \max_e v_e$.

E.7 PENALTY SWEEP (CHOOSING M)

Choose the smallest M in a short sweep $M \in \{M_0, 2M_0, 4M_0, \dots\}$ that (a) yields $\approx 0\%$ chain breaks (equalities hold at minima) and (b) does not degrade best energy. Excessively large M can drown the problem signal.

E.8 FULL PIPELINE

756

758

759

760

761762763

764 765

766

767 768

769

770 771

772773774

775776777

NOTATION HELPERS

- ANNEAL $(Q, q, c; \text{ reads}, \text{gauges}) \rightarrow (E_{\min}, x_{\min}).$
- BUILDMODEL $(Q, q, c, p, S, M, \text{policy}) \rightarrow (Q', q', c', \text{ancillas})$: strict 1D NN model with kept, S embedded via equation 22–equation 23, others pruned by policy.
- CHAINLEN $(e, p) = L_e$.
- CANDIDATES(\mathbb{E}_{far}, S, m): the m far edges with largest Q_{ij} not in S.

```
778
             Algorithm 2 Annealer-Guided 2D-QUBO → Strict 1D NN QUBO (Greedy Selection)
779
             Require: (Q, q, c), line order p, budget K, seed M_0, policy \in \{\text{drop}, \text{fold}\}, anneal settings
780
             Ensure: Final (Q', q', c'), (x_{\text{final}}, E_{\text{final}}), selected set S
781
              1: (E^*, x^*) \leftarrow Anneal(Q, q, c; reads_{ref}, gauges_{ref}) Reference optimum
              2: Partition edges into and \mathbb{E}_{far} using p
782
783
              3: S \leftarrow \varnothing, B \leftarrow 0, M \leftarrow M_0
              4: (Q_0, q_0, c_0, \bot) \leftarrow \text{BUILDMODEL}(Q, q, c, p, S, M, \text{policy})
784
              5: (E_S, \_) \leftarrow \text{ANNEAL}(Q_0, q_0, c_0; \text{ reads}_{\text{score}}, \text{ gauges}_{\text{score}})
785
              6: while B < K \operatorname{do}
786
                      \mathcal{C} \leftarrow \text{CANDIDATES}(\mathbb{E}_{far}, S, m)
787
                      (\Delta^{best}, e^{best}, E^{best}) \leftarrow (0, \perp, \infty)
              8:
788
                      for e \in \mathcal{C} do
              9:
789
             10:
                          L \leftarrow \mathsf{CHAINLEN}(e, p)
790
                          if B+L>K then
             11:
791
                             continue
792
                          end if
             12:
793
                          (Q_e, q_e, c_e, \bot) \leftarrow \text{BUILDMODEL}(Q, q, c, p, S \cup \{e\}, M, \text{policy})
             13:
794
             14:
                          (E_{S \cup \{e\}, -}) \leftarrow \text{ANNEAL}(Q_e, q_e, c_e; \text{ reads}_{\text{score}}, \text{ gauges}_{\text{score}})
                          g \leftarrow \frac{E_S - E_{S \cup \{e\}}}{2}
             15:
796
                                    \max(L,1)
797
                          if g > \Delta^{best} then
             16:
                              (\Delta^{best}, e^{best}, E^{best}) \leftarrow (g, e, E_{S \cup \{e\}})
798
             17:
799
             18:
800
             19:
                      end for
                      if e^{best} = \bot or \Delta^{best} \le \varepsilon then
             20:
801
                          break
802
             21:
                      end if
803
                      S \leftarrow S \cup \{e^{best}\}, \quad B \leftarrow B + ChainLen(e^{best}, p), \quad E_S \leftarrow E^{best}
             22:
804
             23: end while
805
             24: M \leftarrow \text{PENALTYSWEEP}(Q, q, c, p, S, \text{policy}, \{M_0, 2M_0, 4M_0, \dots\})
806
             25: (Q', q', c', \_) \leftarrow \text{BUILDMODEL}(Q, q, c, p, S, M, \text{policy})
807
             26: (E_{\text{final}}, x_{\text{final}}) \leftarrow \text{ANNEAL}(Q', q', c'; \text{reads}_{\text{final}}, \text{gauges}_{\text{final}})
808
809
             28: return (Q', q', c'), (x_{\text{final}}, E_{\text{final}}), S
```

Algorithm 3 One-Shot Selection via Annealed Values + Knapsack

Require: (Q, q, c), line order p, budget K, seed M_0 , policy $\in \{\text{drop}, \text{fold}\}\$

Ensure: Selected set S and final model (Q', q', c')

- 1: $(E^*, x^*) \leftarrow \text{ANNEAL}(Q, q, c)$
- 2: Build base strict 1D NN model (keep, prune \mathbb{E}_{far} per policy); $(E_{\varnothing}, _) \leftarrow \text{ANNEAL}(\text{base})$
- 3: **for** each $e = (i, j) \in \mathbb{E}_{far}$ **do**
- 4: Build "base + embed e with M_0 "; $(E_{\{e\}}, _) \leftarrow \text{ANNEAL}$
- 5: $v_e \leftarrow E_{\varnothing} E_{\{e\}}; \quad L_e \leftarrow pos(i) pos(j) 1$
- 6: end for

- 7: Solve knapsack equation 27 (or QUBO equation 28) to get S
- 8: $M \leftarrow \text{PENALTYSWEEP}(Q, q, c, p, S, \text{policy}, \{M_0, 2M_0, 4M_0, \dots\})$
- 9: Build final strict 1D NN model (embed all $e \in S$ with M; keep; prune others)
- 10: **return** (Q', q', c'), and then $(x_{\text{final}}, E_{\text{final}}) \leftarrow \text{ANNEAL}(Q', \hat{q'}, \hat{c'})$

F TIME COMPLEXITY OF ISING SOLVERS: FORMAL MEASURES AND $O(\cdot)$ SCALINGS

Problem setting. Let G = (V, E) be a graph with |V| = n spins $s_i \in \{\pm 1\}$, couplings J_{ij} , and (optional) fields h_i . We minimize the Ising energy

$$E_{\text{Ising}}(s) = -\frac{1}{2} \sum_{i,j} J_{ij} s_i s_j - \sum_i h_i s_i.$$
 (29)

Computing a ground state is NP-hard in general (e.g., for 3D lattices, and for planar graphs with fields) Barahona (1982).

F.1 What we mean by "time complexity" for Heuristic Ising solvers

For solvers whose single run of duration τ succeeds with probability $p(\tau)$ on a given instance, a device/algorithm-agnostic metric is the *time-to-solution (TTS)* for target confidence $1 - \delta$:

$$_{1-\delta} = \min_{\tau>0} \tau \frac{\log \delta}{\log(1-p(\tau))} . \tag{30}$$

This is the standard "repeat–until–success" model used in annealing benchmarks; the optimization over τ emphasizes that *per-size* schedules must be tuned Rønnow et al. (2014). For Monte Carlo algorithms we count time in *Monte Carlo sweeps* (MCS; cf. one attempted update per spin), then convert to wall time by the measured seconds per sweep.

Two analytic lenses connect equation 30 to exact mathematical quantities. First, for reversible Markov chains (SA and SQA at fixed control parameter), the *mixing time* $t_{mix}(\varepsilon)$ obeys

$$t_{\text{mix}}(\varepsilon) \le \frac{1}{\gamma} \log \frac{1}{\varepsilon \pi_{\text{min}}},$$
 (31)

where γ is the spectral gap and π_{\min} is the minimum stationary probability (Levin et al., 2017, Thm. 20.6). Second, for closed-system QA (adiabatic evolution) the runtime T needed for error $\leq \varepsilon$ satisfies the gap-controlled bound

$$T = O\left(\frac{\max_{s \in [0,1]} \left\| \frac{dH}{ds} \right\|}{\varepsilon \Delta_{\min}^2}\right), \tag{32}$$

with Δ_{\min} the minimum instantaneous spectral gap along the anneal path H(s) Jansen et al. (2007); Albash & Lidar (2018).

F.2 ALGORITHM-BY-ALGORITHM FORMULATIONS

(1) Simulated Annealing (SA). SA runs a temperature-dependent (often single-spin Metropolis) Markov chain with a cooling schedule $T_k \downarrow 0$. A precise convergence criterion is given by Hajek: if

$$T(k) = \frac{c}{\log(1+k)} \quad \text{with} \quad c \ge d^*, \tag{33}$$

then the algorithm converges in probability to the set of global minima; here d^* is the *depth* of the deepest non-global local minimum (a barrier-height functional) Hajek (1988).

At fixed temperature T, the chain's mixing time obeys equation 31; running an anneal that stays near equilibrium yields the upper bound

$$_{1-\delta}^{\mathrm{SA}} = O\left(\sum_{k=1}^{K^*} \frac{1}{\gamma(T_k)} \log \left(\frac{1}{\varepsilon_k \, \pi_{\min}(T_k)}\right)\right), \tag{34}$$

for a quasi-static schedule $\{T_k\}_{k\leq K^*}$ and per-stage accuracies ε_k determined by the schedule discretization.

Empirical example. On random Chimera graphs with ± 1 couplings and optimized anneal times, SA exhibits $= \exp(\Theta(\sqrt{N}))$ scaling (Rønnow et al., 2014, Fig. 3).

(2) Simulated Quantum Annealing (SQA). SQA uses path-integral QMC to sample the Gibbs state of a stoquastic transverse-field Ising Hamiltonian; the Markov chain evolves on an expanded state space of $n \times L$ spins (with L Trotter slices). At a fixed (β, Γ) , the *PIMC* chain's mixing time $t_{\rm mix}^{\rm PIMC}$ controls runtime:

where $\operatorname{nnz}(G)$ counts spin–spin couplers actually touched per sweep. There are families where $t_{\min}^{\operatorname{PIMC}}$ is *provably polynomial*, e.g., 1D stoquastic Hamiltonians at $\beta = O(\log n)$ Crosson & Harrow (2021), and the "spike" cost function where SA is exponentially slow but SQA finds the optimum in $\operatorname{poly}(n)$ time Crosson & Harrow (2016). *Empirical example*. On the same random Chimera benchmarks as above, optimized SQA also exhibits $= \exp(\Theta(\sqrt{N}))$ scaling Rønnow et al. (2014).

(3) Quantum Annealing (QA; adiabatic algorithm / analog devices). For a Hamiltonian path $H(s) = (1-s)H_0 + sH_1$, the adiabatic theorem yields the gap-based complexity in equation 32. Thus.

$$\frac{QA}{1-\delta} = O\left(\frac{\|\dot{H}\|_{\infty}}{\varepsilon \Delta_{\min}^2}\right) \quad \text{(ideal closed system)}$$
(36)

(up to smoothness constants), so exponentially small Δ_{\min} implies exponential time. There are random NP-complete families (e.g., Exact Cover) where Δ_{\min} is exponentially small with high probability, hence adiabatic QA requires exponential time Altshuler et al. (2010). For hardware experiments, one computes TTS exactly as in equation 30 using the per-run anneal time and observed success p Rønnow et al. (2014).

(4) Simulated Bifurcation (SB). SB integrates a classical time-dependent Hamiltonian flow on variables (x_i, y_i) with forces

$$f_i = \sum_j J_{ij} u_j, \qquad u_j = \begin{cases} x_j & \text{(ballistic SB)}, \\ \operatorname{sgn}(x_j) & \text{(discrete SB)}. \end{cases}$$
 (37)

Per time step, the dominant arithmetic is applying J to u, i.e.,

$$cost/step = O(nnz(J))$$
 (sparse) or $O(n^2)$ (dense). (38)

SB papers report a *step-to-solution* (StS) metric that is independent of machine speed: if N_s steps are taken per trial and P is the per-trial success probability, then

$$\boxed{ \operatorname{StS}_{1-\delta} \ = \ N_s \, \frac{\log \delta}{\log (1-P)} } \,, \qquad {}^{\operatorname{SB}}_{1-\delta} \ = \ \operatorname{StS}_{1-\delta} \times (\mathsf{time/step}). \tag{39}$$

Heated/discrete variants reduce StS on Sherrington–Kirkpatrick (dense) benchmarks Kanao & Goto (2022); see Goto et al. (2019; 2021) for the original dynamics and high-performance variants.

¹In the worst case d^* can grow with n, so schedules meeting equation 33 can imply super-polynomial runtime on typical NP-hard families; cf. Barahona (1982).

F.3 SIDE-BY-SIDE SUMMARY (DOMINANT TERMS)

Method	Asymptotic lens for $_{1-\delta}$
SA	$O\!\!\left(\sum_k \gamma(T_k)^{-1} \log_{\frac{\varepsilon_k \pi_{\min}(T_k)}{\varepsilon_k}}\right)$ for a quasi-static schedule;
	converges if $T(k) = c/\log(1+k)$ with $c \ge d^*$ (barrier depth) Hajek (1988); Levin et al. (2017).
SQA	$O(t_{\mathrm{mix}}^{\mathrm{PIMC}}(n, \beta, \Gamma) \cdot \log \frac{1}{\delta})$ with per-sweep $O(\mathrm{nnz}(G)L)$;
	polynomial on certain families (e.g. 1D stoquastic, spike). Crosson & Harrow (2021; 2016)
QA	$O(\ \dot{H}\ _{\infty}/(\varepsilon \Delta_{\min}^2))$ (adiabatic bound); small gaps \Rightarrow exponential time. Jansen et al. (2007); Albash & Lidar (2018)
SB	$StS_{1-\delta} \times$ (time/step), with StS in equation 39 and cost/step in equation 38. Kanao & Goto (2022); Goto et al. (2019)

Practical note. When reporting complexity empirically, optimize schedule/parameters *per* size n and quote $_{1-\delta}$ from equation 30; failure to re-optimize can mask speedups/slowdowns Rønnow et al. (2014).